

Thermodynamic and kinetic properties of the reaction $\text{Cl} + \text{O}_2 + \text{M} = \text{ClOO} + \text{M}$ in the range 160–300 K and 1–1000 bar

S. Baer, H. Hippler, R. Rahn, M. Siefke, N. Seitzinger, and J. Troe

Citation: *The Journal of Chemical Physics* **95**, 6463 (1991); doi: 10.1063/1.461543

View online: <http://dx.doi.org/10.1063/1.461543>

View Table of Contents: <http://scitation.aip.org/content/aip/journal/jcp/95/9?ver=pdfcov>

Published by the [AIP Publishing](#)

Articles you may be interested in

Temperature and pressure dependence of ozone formation rates in the range 1–1000 bar and 90–370 K
J. Chem. Phys. **93**, 6560 (1990); 10.1063/1.458972

ESR investigation of the photoisomerization of OClO to ClOO in an H₂SO₄ glass: Magnetophotoselection and kinetics

J. Chem. Phys. **85**, 2692 (1986); 10.1063/1.451026

Kinetic studies of the reaction of the SO radical with NO₂ and ClO from 210 to 363 K

J. Chem. Phys. **84**, 4371 (1986); 10.1063/1.450059

The kinetics of the reaction of OH with ClO

J. Chem. Phys. **78**, 1140 (1983); 10.1063/1.444906

Kinetics of the reactions of ClO with O and with NO

J. Chem. Phys. **66**, 3673 (1977); 10.1063/1.434403



Thermodynamic and kinetic properties of the reaction $\text{Cl} + \text{O}_2 + M \rightleftharpoons \text{ClOO} + M$ in the range 160–300 K and 1–1000 bar

S. Baer,^{a)} H. Hippler, R. Rahn,^{b)} M. Siefke, N. Seitzinger,^{c)} and J. Troe
*Institut für Physikalische Chemie der Universität Göttingen, Tammannstrasse 6,
D-3400 Göttingen, Germany*

(Received 13 May 1991; accepted 17 July 1991)

The reaction $\text{Cl} + \text{O}_2 + M \rightleftharpoons \text{ClOO} + M$ was studied by laser flash photolysis in the bath gases $M = \text{He}, \text{Ar}, \text{N}_2$, and O_2 over the temperature range 160–300 K and the pressure range 1–1000 bar. UV absorptions of ClOO were monitored, a maximum absorption cross section of $\sigma(248 \text{ nm}) = 3.4 \times 10^{-17} \text{ cm}^2$ was determined. An expression for the equilibrium constant $K_p = 5.3 \times 10^{-6} \exp(+23.4 \text{ kJ mol}^{-1}/RT) \text{ bar}^{-1}$ was derived between 180 and 300 K, which, by a third law analysis, yields $\Delta H_0^\circ = -20.2 \pm 0.2 \text{ kJ mol}^{-1}$. Limiting low pressure rate coefficients for Cl + O₂ recombination of $k_0 = [\text{He}] 8.8 \times 10^{-34} (\text{T}/300 \text{ K})^{-3.0}$, $k_0 = [\text{O}_2] 1.6 \times 10^{-33} (\text{T}/300 \text{ K})^{-2.9}$, $k_0 = [\text{N}_2] 1.4 \times 10^{-33} (\text{T}/300 \text{ K})^{-3.9} \text{ cm}^6 \text{ s}^{-1}$ were obtained over the range 160–260 K, as well as $k_0(160 \text{ K}) = [\text{Ar}] 2.2 \times 10^{-32} \text{ cm}^6 \text{ s}^{-1}$. Rate constants for the reactions $\text{Cl} + \text{ClOO} \rightarrow \text{Cl}_2 + \text{O}_2$ or 2ClO , $\text{ClOO} + \text{ClOO} \rightarrow \text{products}$, and $\text{ClOO} + \text{Cl}_2 \rightarrow \text{Cl}_2\text{O} + \text{ClO}$ were also derived. The recombination $\text{Cl} + \text{O}_2(+M) \rightarrow \text{ClOO}(+M)$ at pressures above 10 bar shows a transition to a high pressure plateau and, at pressures above 200 bar, to diffusion control. It is suggested that, like $\text{O} + \text{O}_2(+M) \rightarrow \text{O}_3(+M)$, the reaction is governed by a radical complex mechanism.

I. INTRODUCTION

The importance of chlorine and chlorine oxides in the chemistry of the stratosphere is well established.¹ In this context, ClOO has been implicated as a short-lived precursor to ClO, which is known to play a crucial role in the ozone destruction cycle.^{2,3} ClOO has proved to be somewhat elusive due to its very weak bonding energy: the Cl–OO bond strength is less than 25 kJ mol^{-1} . The vibrational modes of ClOO were first characterized by Arkell and Schwager,⁴ who photolyzed OClO in an argon matrix. Johnston *et al.*⁵ generated ClOO by photolysis of Cl₂ in the presence of O₂,



and succeeded in detecting its UV absorption spectrum. Kinetic information on reactions (1a) and (1b) has been sparse. Reaction (1b) usually is very fast and ClOO also reacts with residual Cl and with itself. Two studies report rate constants for reaction (1): A value of $k_{1,0} = [\text{Ar}] 5.6 \times 10^{-34} \text{ cm}^6 \text{ s}^{-1}$ near 300 K was obtained by Clyne and Coxon,⁶ a value of $[\text{N}_2 + \text{O}_2] 1.7 \times 10^{-33} \text{ cm}^6 \text{ s}^{-1}$ by Nicholas and Norrish.⁷ In these studies, the ClOO radical was not observed directly; several assumptions had to be made in order to extract reaction rate constants. A summary of the sparse information available led to a recommended value of $k_{1,0} = [0.8\text{N}_2 + 0.2\text{O}_2] 2.7 \times 10^{-33} (\text{T}/300 \text{ K})^{-1.5} \text{ cm}^6 \text{ s}^{-1}$.⁸ Only very recently a direct measurement under stratospheric conditions by Nicovich *et al.*⁹ was reported, which gave $k_{1,0} = [\text{O}_2] 8.9 \times 10^{-33} \text{ cm}^6 \text{ s}^{-1}$ at 187 K. An

equilibrium constant was also determined and a value of the Cl–OO bond energy of 19.9 kJ mol^{-1} was derived.

In the present paper, we describe a more thorough study of the thermodynamic and kinetic properties of reactions (1) and (1a) over the temperature range 160–300 K. Absolute measurements of the UV absorption coefficients of ClOO were made and the rates of formation and subsequent decay of ClOO under stratospheric conditions were measured. Furthermore, falloff curves (between 1 and 1000 bar) of reaction (1) were studied in three different bath gases at 160 K. The implications of our results for the potential role of ClOO in the stratosphere are also discussed.

The present study, was of interest under more general aspects. Our recent study¹⁰ of the recombination $\text{O} + \text{O}_2 + M \rightarrow \text{O}_3 + M$ over the temperature range 90–400 K and at pressures between 1–1000 bar showed anomalous pressure and temperature dependences of the rate coefficients. These observations suggested marked contributions from the radical-complex mechanism in a polyatomic recombination reaction (such as that proposed in Ref. 11) as well as a participation of metastable excited electronic states influenced by cluster effects. It appeared attractive to investigate whether similar phenomena became apparent in the recombination $\text{Cl} + \text{O}_2 + M \rightarrow \text{ClOO} + M$ as well.

II. EXPERIMENTAL TECHNIQUE

Our experiments were performed in a high pressure reaction cell that could be cooled (or heated) over a wide temperature range. This experimental setup has been described previously;¹⁰ only details relevant to the present experiments will be discussed here.

Formation of ClOO was achieved using laser flash photolysis. Cl radicals were formed by the photolysis of Cl₂ at

^{a)} Present address: University of British Columbia, Vancouver, Canada.

^{b)} Present address: BASF, Ludwigshafen, Germany.

^{c)} Present address: U.S. Pharmacopeial Convention, Inc., Rockville, Maryland 20852.

308 nm using an XeCl excimer laser (LPX 100 Lambda Physik, pulse energy 220 mJ, pulse width 40 ns). At 308 nm, Cl is produced predominantly in its ground state, $^2P_{3/2}$; ^{12,13} contributions from $^2P_{1/2}$ were not considered. The photolysis light was combined with the analysis light by means of dielectric mirrors and passed collinearly through the cylindrical reaction cell.

The progress of the reaction was monitored by observing the absorption signal of ClOO at 248 nm. A Hg–Xe high pressure arc lamp (200 W Ushio UXM-200 H) was used as the light source. Generally, the lamp was used in the continuous mode; an electromagnetic shutter admitted the analysis light to the cell shortly before the laser pulse. When only small amounts of Cl_2 were used, it was necessary to pulse the lamp for 80 μs . This produced an intensity gain of a factor of 100, considerably improving the signal-to-noise ratio. Absorption-time signals were recorded using a monochromator (Zeiss MM3), photomultiplier (RCA 1P28A), and digital storage oscilloscope arrangement (LeCroy 9400, bandwidth 125 MHz). When possible, single shots were employed in order to minimize buildup and possible interference of chlorine oxide products. Under conditions of low Cl_2 concentrations, however, the poor signal-to-noise ratio necessitated signal averaging of up to 20 shots. In these cases, the first and last shots were checked for consistency.

At high O_2 pressures, contributions from the O_2 dimer had to be considered. Since the O_2 dimer absorbs at 248 nm¹⁴ this may decrease the transmitted analysis light before the laser pulse, and therefore lead to a decrease in the signal-to-noise ratio. The observed recombination and decay rate constants of ClOO, however, were found to be independent of this effect.

The bath gases He, Ar, and N_2 were obtained from Messer–Griesheim being of purity better than 99.998%. Oxygen and other impurities were removed by a gas cleaning adsorber (Oxisorb, Messer–Griesheim). The bath gases were passed through a 3 μ steel dust filter into an oil-free diaphragm compressor (MK 3000, Nova Swiss) and compressed up to 1 kbar. The reagent gases O_2 and Cl_2 from Messer–Griesheim were of purities better than 99.995% and 99.9%.

Special consideration had to be given to proper gas mixing when high bath gas pressures were applied. All high pressure reaction mixtures were prepared in the cell at room temperature to ensure proper mixing. After waiting for 15–20 min, they were cooled to the appropriate conditions. The photolysis experiments were made only after additional waiting for 30 min at low temperature conditions. Complete mixing was achieved in this way, such as confirmed by controlling the transmission before and after addition of the gases.

III. EXPERIMENTAL RESULTS AND DATA ANALYSIS

A. Formation and decay of ClOO

The reaction scheme for the chlorine/oxygen system is complex. ClOO formation, first, is governed by reactions (1) and (1a). Once formed, ClOO can react with Cl forming Cl_2 and O_2 as well as ClO in reactions (2a) and (2b),^{5,8,15} or

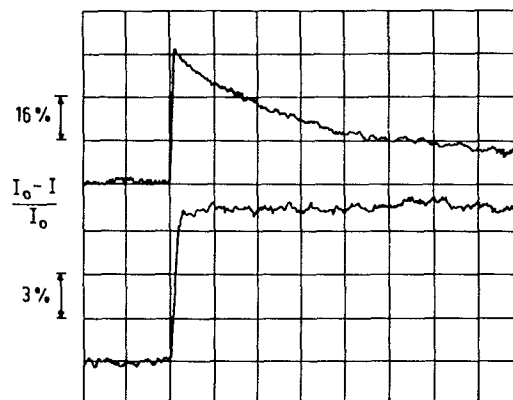


FIG. 1. Upper trace: Absorption-time profile of ClOO formation and decay recorded at 248 nm [$T = 300$ K, $P(\text{Cl}_2) = 5.5$ Torr, $P(\text{O}_2) = 100$ bar, $I_0 =$ incident light intensity, $I =$ transmitted light intensity, excitation at 308 nm with 20 mJ cm^{-2}]. Lower trace: ozone absorption at 265 nm after photolysis of 5.5 Torr of NO_2 in 50 bar O_2 , excitation at 308 nm with 20 mJ cm^{-2} .

it can react with itself forming higher chlorine oxides in reaction (3),



The recombination (4) of Cl forming Cl_2 ,



under the present conditions can be neglected.¹⁶

Formation and disappearance of ClOO at high oxygen pressures occur on distinctly different time scales, such as illustrated in the upper traces of Fig. 1. First, the equilibrium between reaction (1) and (1a) is rapidly established. The relaxation toward this equilibrium, under excess oxygen, follows a rate law

$$\frac{d([\text{ClOO}]_{\text{max}} - [\text{ClOO}])}{dt} = -k_{I,\text{exp}}([\text{ClOO}]_{\text{max}} - [\text{ClOO}]), \quad (5)$$

with

$$k_{I,\text{exp}} = k_1[M](1 + K_{\text{eq}}[\text{O}_2])/K_{\text{eq}}, \quad (6)$$

where K_{eq} is defined by $K_{\text{eq}} = k_1/k_{-1}$. At 300 K and 1 bar of O_2 , this expression corresponds to a relaxation time of about 40 ns. This fast relaxation is then followed by a much slower second-order decay in the ClOO signal, corresponding to the loss of ClOO through reactions (2) and (3). Assuming that the two stages of reaction can be separated, the decay follows a rate law

$$\frac{d[\text{ClOO}]}{dt} = -2k_{II,\text{exp}}[\text{ClOO}]^2, \quad (7)$$

with

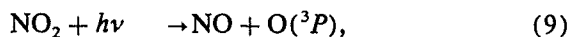
$$k_{II,\text{exp}} = (k_2/K_{\text{eq}}[\text{O}_2] + k_3)/(1 + 1/K_{\text{eq}}[\text{O}_2]), \quad (8)$$

which is derived from $d([\text{ClOO}] + [\text{Cl}])/dt$ with the equilibrium condition between reaction (1a) and (1b). At 300 K and 1 bar of O_2 , this yields a decay half-life greater than 2 μs .

The separability of the two stages of reaction was always controlled by simulation of the complete mechanism.

B. Absorption spectrum of ClOO

The absorption spectrum of ClOO between 240 and 300 nm was investigated by monitoring the maximum extinction of ClOO after the photolysis of 5.5 Torr Cl_2 in the presence of 100 bar of O_2 at 300 K. The total number of photons absorbed was calibrated actinometrically by monitoring ozone formation via



and using absorption cross sections of O_3 from Ref. 17 and quantum yields of NO_2 photolysis from Refs. 18 and 19. The quantum yield of Cl_2 photolysis was assumed to be unity in analogy to I_2 photodissociation.¹² Figure 1 compares the ClOO signal with ozone signals obtained under similar conditions. The room temperature absorption spectrum of ClOO, calibrated in this way, is shown in Fig. 2. The maximum absorption is found near 248 nm, where the absorption cross section σ is equal to $3.4(\pm 0.3) \times 10^{-17} \text{ cm}^2$.

The shape of our ClOO absorption spectrum is in good agreement with that obtained by Johnston *et al.*,⁵ but the cross section differ. A maximum of σ at about 250 nm with $\sigma(250 \text{ nm}) = 1.33 \times 10^{-17} \text{ cm}^2$ was reported in Ref. 5. The discrepancy is partly due to the fact that σ in Ref. 5 was obtained from an inaccurate estimate of the equilibrium constant K_{eq} . If the present value of K_{eq} at 298 K is substituted into the analysis of Ref. 5, a $\sigma(250 \text{ nm}) = 1.8 \times 10^{-17} \text{ cm}^2$ is obtained. The reason for the remaining discrepancy must be searched for in this complicated mechanism and the procedure to extract σ from it. Very recently we learned that a σ value near 250 nm of $3 \times 10^{-17} \text{ cm}^2$ was also obtained in Ref. 20, confirming the present results.

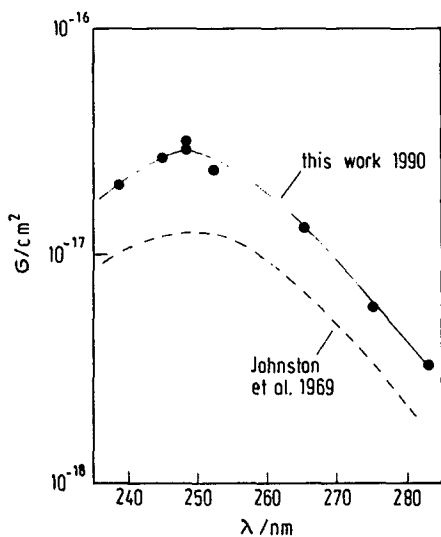


FIG. 2. Absorption spectrum of ClOO.

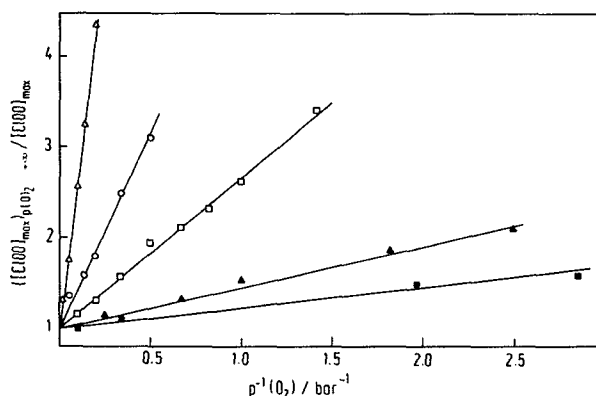


FIG. 3. Dependence of ClOO maximum yields on the oxygen pressure (■: $T = 200 \text{ K}$; ▲: $T = 220 \text{ K}$; □: $T = 240 \text{ K}$; ○: $T = 260 \text{ K}$; and △: $T = 300 \text{ K}$).

C. Equilibrium constant for $\text{Cl} + \text{O}_2 \rightleftharpoons \text{ClOO}$

The equilibrium constant K_{eq} , i.e.,

$$K_{\text{eq}} = [\text{ClOO}] / [\text{Cl}][\text{O}_2] \quad (11)$$

is obtained in the following way. In a series of experiments at constant temperature, the quantity $[\text{Cl}]_{t=0}$ of photolyzed chlorine was kept constant and the oxygen pressure was varied. From the ClOO maximum absorption then K_{eq} was obtained through the relationship

$$([\text{ClOO}]_{\text{max}})_{[\text{O}_2] \rightarrow \infty} / [\text{ClOO}]_{\text{max}} = 1 + 1/K_{\text{eq}} [\text{O}_2], \quad (12)$$

where $([\text{ClOO}]_{\text{max}})_{[\text{O}_2] \rightarrow \infty} = [\text{Cl}]_{t=0}$ corresponds to the intercept of a $1/[\text{ClOO}]_{\text{max}}$ vs $1/[\text{O}_2]$ plot. The determination of K_{eq} from the slope of this plot is independent of the ClOO absorption coefficient. Here K_{eq} was obtained in this manner for a series of temperatures between 180 and 300 K. Figure 3 shows the corresponding experimental results.

A van t'Hoff plot of the corresponding values of K_p is given in Fig. 4. The results of Fig. 4 were further evaluated

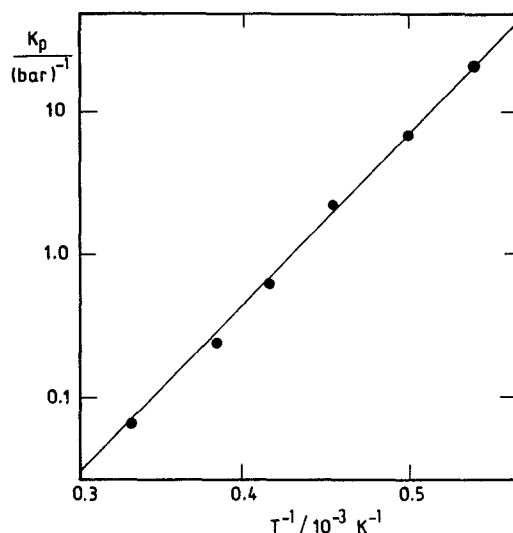


FIG. 4. Van t'Hoff plot of the equilibrium constant $K_p [K_p = P(\text{ClOO})/P(\text{O}_2)P(\text{Cl})]$; ●: experimental points; full line = third-law fit to the points; see the text).

TABLE I. Thermodynamic properties of ClOO (C_p^0 , S^0 , and $-[G^0 - H_{298}^0]/T$ in $\text{J K}^{-1} \text{mol}^{-1}$; H_{298}^0 , ΔH_f^0 , $\Delta_f G^0$ in kJ mol^{-1} ; $\log K_p$ corresponds to the reaction of formation $1/2 \text{Cl}_2 + \text{O}_2 \rightarrow \text{ClOO}$, K_p being given in $\text{bar}^{-1/2}$).

T/K	C_p^0	S^0	$-[G^0 - H_{298}^0]/T$	$H^0 - H_{298}^0$	$\Delta_f H^0$	$\Delta_f G^0$	$\log K_p$
0	0.000	0.000	inf.	-11.602	99.128	99.128	inf.
100	35.196	224.844	307.264	-8.242	98.128	102.425	-53.503
200	42.246	251.538	273.284	-4.349	97.591	106.977	-27.940
250	44.518	261.220	269.930	-2.177	97.496	111.705	-23.340
298	46.154	269.182	269.183	0.000	97.457	111.613	-19.565
300	46.216	269.491	269.184	0.092	97.317	111.562	-19.425

employing a third-law analysis. Here ΔS^0 values were calculated using data from the JANAF tables²¹ and ClOO frequencies of 373, 407, 1441 cm^{-1} from Ref. 4. The moments of inertia were calculated with the geometry given in Ref. 4, i.e., $r(\text{Cl}-\text{O}) = 1.83 \text{ \AA}$, $r(\text{O}-\text{O}) = 1.23 \text{ \AA}$, and $\alpha(\text{ClOO}) = 110^\circ$. The best fit to the experimental data then was obtained with $\Delta H^0(0 \text{ K}) = -20.2 \text{ kJ/mol}$. The third-law fit of the experimental equilibrium constants is included in Fig. 4. It corresponds to an expression

$$K_p = 5.3 \times 10^{-6} \exp(+23.4 \text{ kJ mol}^{-1}/RT) \text{ bar}^{-1}. \quad (13)$$

Our equilibrium constant at 185.4 K of $K_p = 20.7 \text{ bar}^{-1}$ agrees very well with the value of $K_p = 18.9 \text{ atm}^{-1}$ recently derived by Nicovich *et al.*⁹ Likewise, the third-law values of ΔH_0^0 from this work ($\Delta H_0^0 = -20.2 (\pm 0.2) \text{ kJ mol}^{-1}$, obtained from measurements over the temperature range 180–300 K) and of Ref. 9 ($\Delta H_0^0 = -19.9 (\pm 2.0) \text{ kJ mol}^{-1}$, obtained from measurements near 186 K) agree well. We tabulate the corresponding thermodynamic properties of ClOO in Table I.

D. Rate constants for ClOO decay

At temperatures below 260 K, the ClOO decay follows a clean second-order law (see Fig. 5). The apparent second-order rate coefficients are evaluated by analogy to Eq. (8), i.e., by plots of

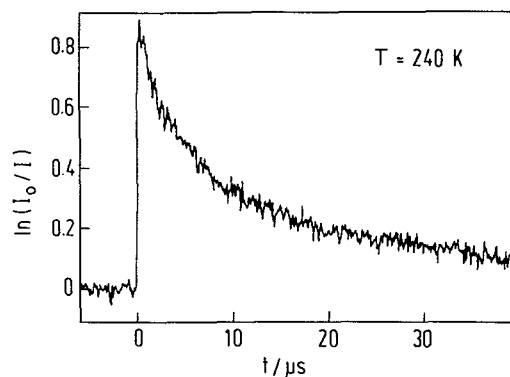


FIG. 5. Absorption-time profile of ClOO decay at $T = 240 \text{ K}$ (observation at 248 nm, photolysis at 308 nm of 5.5 Torr of Cl_2 in 50 bar of O_2).

$k_{\text{II,exp}} [1 + 1/K_p P(\text{O}_2)] = k_2/K_p P(\text{O}_2) + k_3 \quad (14)$
as a function of $1/K_p P(\text{O}_2)$. The experimental results for temperatures between 180 and 260 K are shown in Fig. 6. Here k_2 and k_3 apparently do not depend on the temperature. The values obtained are $k_2 = 2.7 \times 10^{-10} \text{ cm}^3 \text{ s}^{-1}$ and $k_3 = 1.6 \times 10^{-11} \text{ cm}^3 \text{ s}^{-1}$.

Our present results for k_2 are in fair agreement with earlier measurements summarized in Ref. 8, which suggested $1.4 \times 10^{-10} \text{ cm}^3 \text{ s}^{-1}$ for the $\text{Cl}_2 + \text{O}_2$ channel and $8.0 \times 10^{-12} \text{ cm}^3 \text{ s}^{-1}$ for the 2 ClO channel. The present result of $k_2 = 2.7 \times 10^{-10} \text{ cm}^3 \text{ s}^{-1}$, being based on an independent measurement of the ClOO absorption cross section appears to be more directly obtained than k_2 from the earlier work. Measurements about the ClOO self-reaction (3) apparently have not been reported before.

At 300 K, an additional first-order component in the ClOO decay was observed, such as illustrated in Fig. 7. This decay could no longer be modeled by the scheme of reactions (1)–(3). One might think of a unimolecular isomerization



which is estimated to be 7 kJ mol^{-1} endothermic⁸ and which was suggested²² to occur in solution under photolysis conditions. If the isomerization barrier would be low enough for the reaction to occur near 300 K, one would expect the back reaction to occur as well. In this case, fast equilibration would take place and OCIO would not be a relatively stable

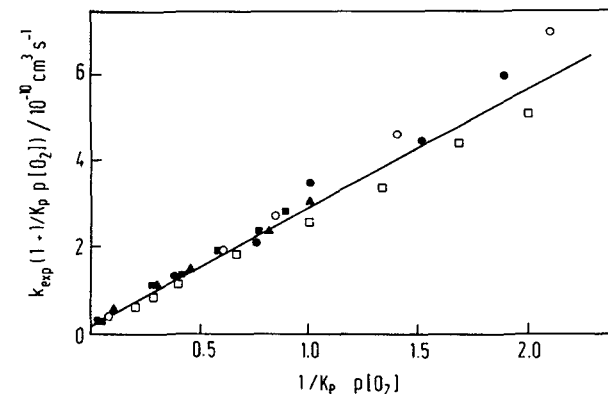


FIG. 6. Analysis of ClOO decay through Eq. (14) (O: $T = 185 \text{ K}$; ■: $T = 200 \text{ K}$; ▲: $T = 220 \text{ K}$; □: $T = 240 \text{ K}$; ○: $T = 260 \text{ K}$).

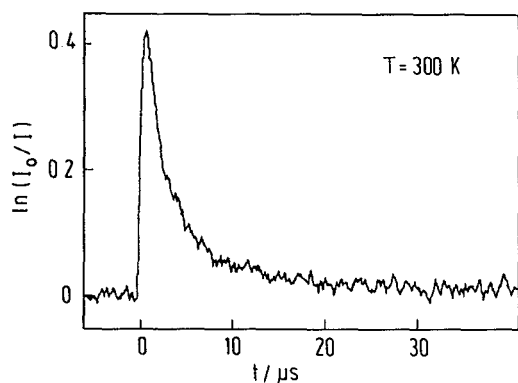


FIG. 7. Absorption-time profile of ClOO decay at $T = 300$ K (conditions as in Fig. 6).

gas at room temperature, as it would decompose very fast via ClOO. Subsequent decomposition of ClOO via a fast reaction with ClO also cannot explain the observed additional first component at room temperature. In that case, ClO would quickly reach a quasistationary state, which immediately would lead to a second-order decay law for ClOO. Instead, a reaction



could act as a sink for ClOO. Unfortunately, experimental constraints did not allow for larger variations of $[\text{Cl}_2]$ in order to test whether the ClOO decay depends on $[\text{Cl}_2]$. Choosing $k_{16} = 3.4 \times 10^{-12} \text{ cm}^3 \text{ s}^{-1}$, we were able to simulate our profiles perfectly well. However, this interpretation of the first-order decay component remains tentative at this moment.

E. Rate constants for ClOO formation

A sample absorption-time profile for ClOO formation at 160 K is shown in Fig. 8. The evaluation of the shown profile with Eqs. (5) and (6) leads to k_1 . As can be seen from Eq. (6), $k_{1,\text{exp}}$ depends directly on the magnitude of the equilib-

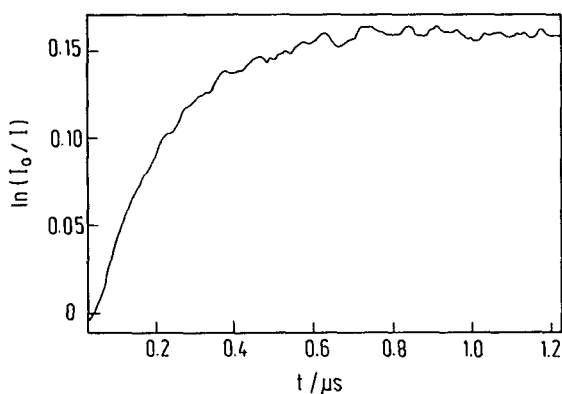


FIG. 8. Absorption-time profile of ClOO formation at $T = 160$ K (observation at 248 nm, photolysis at 308 nm of 1.3 Torr of Cl_2 in 40 Torr of O_2 and 3 bar of N_2).

TABLE II. Second order rate coefficients k_1 for $\text{Cl} + \text{O}_2 + \text{He} \rightarrow \text{ClOO} + \text{He}$ at $T = 160$ K ($D =$ self-diffusion coefficients of the bath gas He).

$[\text{He}]/\text{cm}^{-3}$	$D^{-1}/\text{s cm}^{-2}$	$k_1/\text{cm}^3 \text{ s}^{-1}$
4.2×10^{19}	0.6×10^1	4.2×10^{-13}
1.3×10^{20}	1.8×10^1	7.9×10^{-13}
4.5×10^{20}	6.0×10^1	2.4×10^{-12}
1.3×10^{21}	1.6×10^2	6.4×10^{-12}
3.9×10^{21}	4.6×10^2	2.2×10^{-11}
7.1×10^{21}	7.3×10^2	2.7×10^{-11}
1.2×10^{22}	1.1×10^3	4.9×10^{-11}
3.0×10^{22}	2.1×10^3	3.6×10^{-11}

rium constant K_{eq} . Because the corresponding K_p values range from 20.8 bar^{-1} at 180 K to 0.068 bar^{-1} at 300 K, for given O_2 and M pressures the equilibrium will be much faster attained at higher temperatures than at lower temperatures, while simultaneously the magnitude of the ClOO signal will be much smaller. This introduces an upper limit for the temperature range of k_1 measurements. The lower limit of the accessible temperature range is determined by the vapor pressure of Cl_2 , e.g., 0.4 Torr at 150 K. For these reasons, complete falloff curves for the recombination reaction (1) were only measured at 160 K where $K_p = 200 \text{ bar}^{-1}$ and the vapor pressure of $\text{Cl}_2 = 2$ Torr.

For the bath gases He, N_2 , and Ar, the derived pressure-dependent second-order rate constants, k_1 , at 160 K are summarized in Tables II–IV. Pressures were varied from 1 to 1000 bar. The densities and inverse self-diffusion coefficients D^{-1} of the bath gases are included.²³ Falloff curves of k_1 are shown in Fig. 9. In order to identify transition to diffusion controlled behavior,²⁴ plots with a D^{-1} scale are also shown in Fig. 10.

N_2 and Ar falloff curves look quite similar over the entire observed density range. The curves appear to approach the low pressure limit at $[M] < 10^{21} \text{ cm}^{-3}$. A broad plateau of k_1 over the range $10^{21} \leq [M] \leq 10^{22} \text{ cm}^{-3}$ suggests that a high pressure limit of $k_{1,\infty} \approx 2.7 \times 10^{-11} \text{ cm}^3 \text{ s}^{-1}$ is attained. A decrease of the measured rate coefficients sets in at the highest densities, $[M] > 10^{22} \text{ cm}^{-3}$ perhaps suggesting the onset of diffusion control. The falloff curve for $M = \text{He}$

TABLE III. Second-order rate coefficients k_1 for $\text{Cl} + \text{O}_2 + \text{N}_2 \rightarrow \text{ClOO} + \text{N}_2$ at $T = 260$ K.

$[\text{N}_2]/\text{cm}^{-3}$	$D^{-1}/\text{s cm}^{-2}$	$k_1/\text{cm}^3 \text{ s}^{-1}$
4.5×10^{19}	1.3×10^1	9.0×10^{-13}
1.4×10^{20}	4.1×10^1	2.2×10^{-12}
4.8×10^{20}	1.4×10^2	7.0×10^{-12}
1.5×10^{21}	4.1×10^2	1.9×10^{-11}
4.6×10^{21}	1.3×10^3	2.8×10^{-11}
8.2×10^{21}	2.7×10^3	2.8×10^{-11}
1.5×10^{22}	1.0×10^4	2.6×10^{-11}
1.7×10^{22}	1.4×10^4	2.4×10^{-11}

TABLE IV. Second-order rate coefficients k_1 for $\text{Cl} + \text{O}_2 + \text{Ar} \rightarrow \text{ClOO} + \text{Ar}$ at $T = 160$ K.

$[\text{Ar}]/\text{cm}^{-3}$	$D^{-1}/\text{s cm}^{-2}$	$k_1/\text{cm}^3 \text{ s}^{-1}$
4.6×10^{19}	1.2×10^1	1.1×10^{-12}
9.0×10^{19}	2.3×10^1	1.8×10^{-12}
1.4×10^{20}	3.5×10^1	2.4×10^{-12}
2.3×10^{20}	5.8×10^1	4.3×10^{-12}
4.8×10^{20}	1.2×10^2	7.2×10^{-12}
9.8×10^{20}	2.6×10^2	1.9×10^{-11}
2.4×10^{21}	6.3×10^2	2.2×10^{-11}
4.8×10^{21}	1.4×10^3	2.7×10^{-11}
7.1×10^{21}	2.3×10^3	2.6×10^{-11}
1.2×10^{22}	5.2×10^3	2.5×10^{-11}
1.5×10^{22}	9.0×10^3	2.4×10^{-11}
2.0×10^{22}	1.9×10^4	2.0×10^{-11}

looks strikingly different from that observed for N_2 and Ar . At low densities, the observed rate coefficients k_1 in He are four times smaller than those in N_2 or Ar . The falloff curve for $M = \text{He}$ eventually crosses those of the other two bath gases at densities near $5 \times 10^{21} \text{ cm}^{-3}$. In He, a broad plateau of k_1 is not observed. The difference in Fig. 10 between the onsets of a decay of k_1 at the highest pressures of He, Ar , and N_2 suggests that there is not a simple transition from a high pressure plateau to a diffusion controlled range of k_1 .

Temperature dependences of the limiting low pressure third-order rate constants $k_{1,0}$ were measured for the bath gases He, O_2 , and N_2 . $k_{1,0}$ values are summarized in Table V and illustrated in Fig. 11. The curves all show very strong negative temperature coefficients. The results can be represented by

$$k_{1,0}/[\text{He}] = 8.8 \times 10^{-34} (T/300 \text{ K})^{-3.0} \text{ cm}^6 \text{ s}^{-1} \quad (17)$$

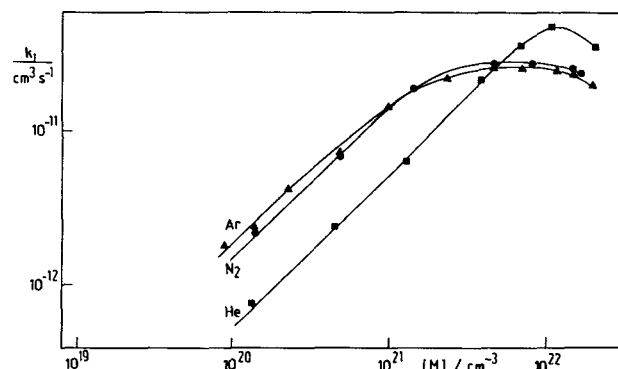
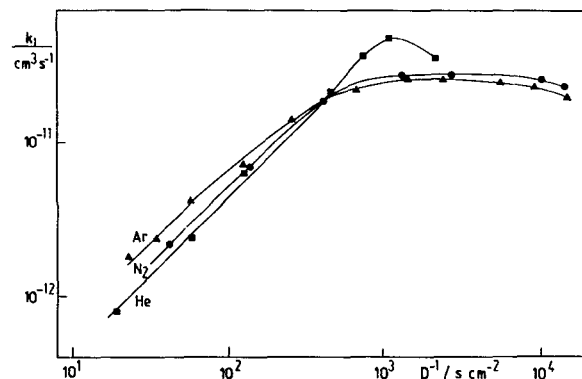
(160–260 K),

$$k_{1,0}/[\text{O}_2] = 1.6 \times 10^{-33} (T/300 \text{ K})^{-2.9} \text{ cm}^6 \text{ s}^{-1} \quad (18)$$

(160–260 K),

$$k_{1,0}/[\text{N}_2] = 1.4 \times 10^{-33} (T/300 \text{ K})^{-3.9} \text{ cm}^6 \text{ s}^{-1} \quad (19)$$

(160–240 K),

FIG. 9. Falloff curves of the recombination $\text{Cl} + \text{O}_2 + M \rightarrow \text{ClOO} + M$ in $M = \text{He}, \text{N}_2$, and Ar at $T = 160$ K.FIG. 10. As in Fig. 9, representation as a function of the inverse of the self-diffusion coefficient D of the bath gas.

$$k_{1,0}/[\text{Ar}] = 2.2 \times 10^{-32} \text{ cm}^6 \text{ s}^{-1} \quad (160 \text{ K}). \quad (20)$$

Our value for $M = \text{O}_2$ and $T = 186.5$ K of $k_{1,0}/[\text{O}_2] = (6.3 \pm 1.2) \times 10^{-33} \text{ cm}^6 \text{ s}^{-1}$ agrees well with that of $k_{1,0}/[\text{O}_2] = (8.9 \pm 2.9) \times 10^{-33} \text{ cm}^6 \text{ s}^{-1}$ from Ref. 9. On the basis of an analysis of systematic errors, we estimate that our measurements of $k_{1,0}/[M]$ have an uncertainty of $\pm 20\%$.

IV. DISCUSSION

In the following we discuss the properties of the measured recombination rate coefficients of the reaction $\text{Cl} + \text{O}_2 \rightarrow \text{ClOO}$, its absolute values and its temperature and pressure dependences. First we consider the low pressure limit of the reaction. If the energy transfer mechanism would apply, the low pressure pseudo-second-order rate coefficient could be expressed in the form

$$k_0 \approx [M] Z_{\text{LJ}} \beta_c (h^2/2\pi\mu kT)^{3/2} \rho_{\text{vib},h}(E_0) kT \quad (21)$$

$$\frac{Q_{\text{rot,el}}(\text{ClOO})}{Q_{\text{vib,rot,el}}(\text{O}_2) Q_{\text{el}}(\text{Cl})} F_e F_{\text{anh}} F_{\text{rot}},$$

with the nomenclature of Ref. 25. The evaluation of Eq. (21) is straightforward. Even taking into account all uncertainties in the input parameters, such as absolute values and temperature dependences of average energies $\langle \Delta E \rangle$ transferred per collision, which enter the collision efficiencies β_c , one

TABLE V. Low pressure rate coefficients $k_{1,0}$ for the reaction $\text{Cl} + \text{O}_2 + M \rightarrow \text{ClOO} + M$ in the range 160–260 K.

T/K	$k_{1,0}/[\text{N}_2] \text{ cm}^6 \text{ s}^{-1}$	$k_{1,0}/[\text{He}] \text{ cm}^6 \text{ s}^{-1}$	$k_{1,0}/[\text{O}_2] \text{ cm}^6 \text{ s}^{-1}$
160	1.6×10^{-32}	5.9×10^{-33}	9.7×10^{-33}
180	1.0×10^{-32}	...	6.8×10^{-33}
200	7.0×10^{-33}	2.9×10^{-33}	5.2×10^{-33}
220	4.2×10^{-33}	2.3×10^{-33}	4.0×10^{-33}
240	3.3×10^{-33}	1.7×10^{-33}	3.0×10^{-33}
260	...	1.3×10^{-33}	2.4×10^{-33}

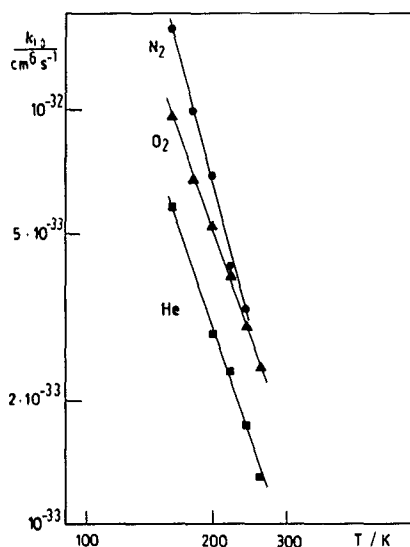
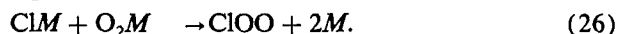


FIG. 11. Limiting low pressure rate coefficients $k_{1,0}$ of the recombination $\text{Cl} + \text{O}_2 + M \rightarrow \text{ClOO} + M$ in $M = \text{He}, \text{O}_2,$ and N_2 .

does not obtain temperature coefficients stronger than about $k_0 \propto T^{-1 \pm 1}$. Furthermore, the measured absolute values of k_0 exceed the calculated values by factors between 10 and 100. For instance, for $T = 160$ K, we calculate low pressure strong collision rate coefficients of $k_{1,0}^{\text{SC}}/[M] = 7.6 \times 10^{-34}, 4.1 \times 10^{-34},$ and $3.6 \times 10^{-34} \text{ cm}^6 \text{ s}^{-1}$ for $M = \text{He}, \text{N}_2,$ and $\text{Ar},$ respectively. In comparison, the corresponding experimental values are $k_{1,0}/[M] = 5.9 \times 10^{-33}, 1.6 \times 10^{-32},$ and $2.2 \times 10^{-32} \text{ cm}^6 \text{ s}^{-1},$ respectively. These effects are even more pronounced than for our earlier low pressure measurements of ozone recombination.¹⁰ Consequently, we conclude that, as in the ozone system, the present recombination reaction is not governed by the energy transfer mechanism but by a radical-complex mechanism. It appears worthwhile mentioning that the present system, because of the very small bond energy and comparably high vibrational frequencies of ClOO, is characterized by an even smaller vibrational density of states than the ozone system. The very small bond energy, which is of the order of those found for hydrogen-bonded complexes, makes this system particularly interesting.

Coming to the conclusion that the energy transfer mechanism is not operating for the present reaction like for $\text{O} + \text{O}_2 \rightarrow \text{O}_3,$ we consider the radical-complex mechanism²⁶



At high pressures, higher complexes will become important as well. In the low pressure limit, this mechanism leads to

$$k_{1,0} = (K_{22}k_{25} + K_{23}k_{24})[M], \quad (27)$$

where K_{22} and K_{23} are equilibrium constants for the complex formations (22) and (23), respectively. To a first approxi-

mation, one may estimate K_{22} and K_{23} by²⁷

$$K \approx \sqrt{\pi} \sigma_{\text{LJ}} (\epsilon_{\text{LJ}}/kT)^{3/2} [8/3 + (32/45)\epsilon_{\text{LJ}}/kT]. \quad (28)$$

The Lennard-Jones parameters ϵ_{LJ} and σ_{LJ} for O_2-M are known²⁸ as $\epsilon_{\text{LJ}}/k = 29,130$ and 125 K and $\sigma_{\text{LJ}} = 3.44, 3.62,$ and 3.66 \AA for $\text{O}_2-\text{He}, \text{O}_2-\text{Ar},$ and $\text{O}_2-\text{N}_2,$ respectively. Unfortunately, only estimated values²⁹ for ϵ_{LJ}/k and σ_{LJ} for $\text{Cl}-M$ are available at this time:³⁰ $\epsilon_{\text{LJ}}/k = 37,110,$ and 97 K and $\sigma_{\text{LJ}} = 3.08, 3.58,$ and 3.71 \AA for $\text{Cl}-\text{He}, \text{Cl}-\text{Ar},$ and $\text{Cl}-\text{N}_2,$ respectively. Using these values for $M = \text{Ar}$ and N_2 at 160 K, Eq. (28) yields $K_{22} \approx K_{23} \approx 1.65 \times 10^{-22} \text{ cm}^3.$ Substituting the experimental values for $k_{1,0},$ Eq. (27) yields $k_{24} + k_{25} \approx 9.5 \times 10^{-11} \text{ cm}^3 \text{ s}^{-1}.$ This implies that k_{24} and k_{25} are close to but somewhat below the Lennard-Jones collision frequencies (e.g., for O_2-Ar one has $Z_{\text{LJ}} \approx 8 \times 10^{-11} \text{ cm}^3 \text{ s}^{-1},$ which does not appear unreasonable. The observation of a markedly smaller $k_{1,0}$ value for $M = \text{He}$ is also consistent with the assumption of a radical-complex mechanism.

The strongest negative temperature coefficient of K compatible with Eq. (28) is $K \propto T^{-2.5},$ which does not appear sufficient to account for the observed values near $k_{-1} \propto T^{-3.4 \pm 0.5}.$ In part this discrepancy may be due to the fact that Eq. (28) is an approximation only. (For more accurate treatments, see Ref. 31). Furthermore, one may think of complications due to the participation of several electronic states of ClOO that correlate with $\text{Cl}(^2P_{3/2})$ and $\text{O}_2(^3\Sigma_g^-).$ Without further speculating at this stage, it appears worth mentioning that the temperature coefficients of $k_{1,0}$ for the present system are similar to those of ozone recombination and that the absolute values are quite similar, being about a factor of 2–3 higher than for the ozone system.

The pressure dependence of the radical complex at high pressures so far is not well understood. There is certainly the formation of larger clusters, such as recognized in trajectory calculations.³² This appearance of larger clusters may result in anomalous falloff behavior, such as summarized in Ref. 33. Ultimately diffusion control sets in. Obviously, a simple relation

$$1/k_1 \approx 1/k_{1,0} + 1/k_{1,\text{diff}} \quad (29)$$

does not describe this transition in the present case. Instead, at least for $M = \text{Ar}$ and N_2 there appears to be broad intermediate plateau that could be described by³³

$$1/k_1 \approx 1/k_{1,0} + 1/k_{1,\infty} + 1/k_{1,\text{diff}}. \quad (30)$$

It appears premature to speculate whether the apparent values of $k_{1,\infty}$ (being close to $3 \times 10^{-11} \text{ cm}^3 \text{ s}^{-1}$ for $M = \text{Ar}$ and N_2) correspond to the high pressure limit of the mechanism (22)–(26) or to something else. The different behavior for $M = \text{He}$ presents a caveat. The markedly more anomalous character of the falloff curves for the ozone system also appear worth mentioning. More theoretical work in this direction appears desirable.

The present results about ClO₂ kinetics and absorption cross sections will change the predictions of its role in stratospheric kinetics to some extent. Given the equilibrium constants of our work, one estimates an equilibrium transformation of Cl into ClOO of 0.3% at $T = 250$ K and $P(\text{O}_2) = 5$ mbar (corresponding to an altitude of 25 km).

At the lower temperatures of the antarctic stratosphere in spring, this transformation will increase: for $T = 185$ K and the same oxygen pressure as above, about 10% of Cl will be transformed into ClOO. The present rate coefficients of reactions (1), (1a), (2), (3), and (16) put ClOO kinetics on a less speculative basis than before.

ACKNOWLEDGMENTS

Financial support of this work by the Deutsche Forschungsgemeinschaft (Sonderforschungsbereich SFB 93 "Photochemie mit Lasern") is gratefully acknowledged.

- ¹For example, see B. J. Finlayson-Pitts and J. N. Pitts, Jr., *Atmospheric Chemistry* (Wiley Interscience, New York, 1986), Part 9.
- ²L. T. Molina and M. J. Molina, *J. Phys. Chem.* **91**, 433 (1987).
- ³R. A. Cox and G. D. Hayman, *Nature* **332**, 796 (1988).
- ⁴A. Arkell and J. Schwager, *J. Am. Chem. Soc.* **89**, 5999 (1967).
- ⁵H. S. Johnston, E. D. Morris, Jr., and J. Van den Borgade, *J. Am. Chem. Soc.* **91**, 7712 (1969).
- ⁶M. A. A. Clyne and J. A. Coxon, *Proc. R. Soc. London, Ser. A* **303**, 207 (1968).
- ⁷J. E. Nicholas and R. G. W. Norrish, *Proc. R. Soc. London Ser. A* **307**, 391 (1968). This is the "preferred" value of Ref. 6.
- ⁸W. B. DeMore, D. M. Golden, R. F. Hampson, C. J. Howard, M. J. Kurylo, M. J. Molina, A. R. Ravishankara, and S. P. Sander, Chemical kinetics and photochemical data for use in stratospheric modeling evaluation number 9, JPL Publication 90, 1988; D. L. Baulch, R. A. Cox, R. F. Hampson, Jr., J. A. Kerr, J. Troe, and R. T. Watson, *J. Phys. Chem. Ref. Data* **18**, 881 (1989).
- ⁹J. M. Nicovich, K. D. Kreutter, C. J. Shackelford, and P. H. Wine, *Chem. Phys. Lett.* (in press).
- ¹⁰H. Hippler, R. Rahn, and J. Troe, *J. Chem. Phys.* **93**, 6560 (1990).
- ¹¹A. E. Croce de Cobos and J. Troe, *Int. J. Chem. Kinet.* **16**, 1519 (1984).
- ¹²H. Okabe, *Photochemistry of Small Molecules* (Wiley Interscience, New York, 1978).

- ¹³G. E. Busch, R. T. Mahoney, R. I. Morse, and K. R. Wilson, *J. Chem. Phys.* **51**, 449 (1969).
- ¹⁴Shardanand, *Phys. Rev.* **186**, 5 (1969).
- ¹⁵R. A. Cox, R. G. Derwent, A. E. J. Eggleton, and H. J. Reid, *J. Chem. Soc. Faraday Trans. 1* **75**, 1648 (1979).
- ¹⁶H. Hippler and J. Troe, *Int. J. Chem. Kinet.* **8**, 501 (1976).
- ¹⁷D. C. Astholz, A. E. Croce, and J. Troe, *J. Phys. Chem.* **86**, 696 (1982).
- ¹⁸H. Gaedtke, H. Hippler, and J. Troe, *Chem. Phys. Lett.* **16**, 177 (1972); H. Gaedtke and J. Troe, *Ber. Bunsenges. Phys. Chem.* **79**, 184 (1975).
- ¹⁹J. N. Pitts, Jr., J. H. Sharp, and S. I. Chan, *J. Chem. Phys.* **42**, 3655 (1964); H. W. Ford and S. Jaffe, *J. Chem. Phys.* **38**, 2935 (1963); I. T. N. Jones and K. D. Bayes, *J. Chem. Phys.* **59**, 4836 (1973).
- ²⁰R. L. Mauldin, J. B. Burkholder, and A. R. Ravishankara (to be published).
- ²¹JANAF Thermochemical Tables, 3rd ed., M. W. Chase, Jr., C. A. Davies, J. R. Downey, Jr., D. J. Frurip, R. A. McDonald, and A. N. Syverud, *J. Phys. Chem. Ref. Data* **14**, Suppl. Nos. 1 and 2 (1985).
- ²²V. Vaida and J. Simon (private communication).
- ²³H. Hippler, V. Schubert, and J. Troe, *Ber. Bunsenges. Phys. Chem.* **89**, 760 (1985).
- ²⁴J. Schroeder and J. Troe, *Annu. Rev. Phys. Chem.* **38**, 163 (1987).
- ²⁵J. Troe, *J. Chem. Phys.* **66**, 4745, 4758 (1977); *J. Phys. Chem.* **83**, 114 (1979).
- ²⁶J. Troe, *Annu. Rev. Phys. Chem.* **29**, 223 (1978), and references included therein.
- ²⁷D. L. Bunker and N. Davidson, *J. Am. Chem. Soc.* **80**, 5090 (1958); deviations from this expression for K are expected for He.
- ²⁸E. Lazzatti, F. Pirani, and F. Vecchiocattivi, *Mol. Phys.* **34**, 1279 (1977); B. Brunetti, B. Luiti, E. Luzzatti, F. Pirani, and F. Vecchiocattivi, *J. Chem. Phys.* **74**, 6734 (1981).
- ²⁹R. A. Svehla, NBS Technical Report R-132, 1963.
- ³⁰Experimental measurements of the interatomic forces of Cl with the rare gases are presently underway; V. Aquilanti, R. Candori, D. Cappelletti, V. Lorent, E. Luzzatti, and F. Pirani, poster presented at the 11th International Symposium on Gas Kinetics, Assisi, Italy, September 1990.
- ³¹P. S. Dardi and J. S. Dahler, *J. Chem. Phys.* **93**, 242 (1990).
- ³²A. J. Stace and J. N. Murrell, *Mol. Phys.* **3**, 1 (1977).
- ³³J. Troe, *Ber. Bunsenges. Phys. Chem.* **95**, 228 (1991), and earlier references cited therein.